Geophys. J. R. astr. Soc. (1972) **28**, 431–458.

Discrimination Between Earthquakes and Underground Explosions Employing an Improved M_S Scale

P. D. Marshall and P. W. Basham

(Received 1972 February 22)

Summary

The M_s Rayleigh wave magnitude formula is revised for purposes of eliminating the heretofore variable effects of near distances and propagation paths on the values computed from standard long-period seismograms. The improved formulation employs a revised distance correction function and a period-dependent path correction that normalizes M_s to large teleseismic distance 20-s values. For purposes of earthquake-explosion discrimination, an empirical focal depth correction is derived on the basis of Rayleigh wave frequency content as a function of focal depth, which normalizes M_s values to the surface focus equivalent, i.e. aids discrimination when it can be applied by increasing earthquake M_s values and moving them away from the equivalent explosion population on $M_s : m_b$ plots. The revised M_s improves on previously achieved discrimination of North American events, and provides reliable discrimination between suites of Eurasian earthquakes and explosions. Having removed the dominant propagation path effects on M_s, the residual differences in $M_s : m_b$ among events are generally attributed to source environment and regional effects on m_b.

The 42 Eurasian WWSSN stations employed are shown to have a discrimination threshold at the $M_s 3{\cdot}2$ level. With the improved M_s scale now equivalent to first order for North American and Eurasian continental propagation, available Nevada Test Site explosion yields are extrapolated to the Eurasian sites to illustrate that this $M_s 3{\cdot}2$ discrimination threshold is equivalent to an Eurasian explosion of about 20 kt in hard rock. Given improved long-period instrumentation to reduce the Rayleigh wave detection threshold, the principal restriction on further studies of discrimination to lower levels of magnitude and yield will be the availability of earthquake occurrence information at the low magnitudes.

1. Introduction

The science of seismology has received great impetus in the last decade because it can play an important role in the detection and identification of underground nuclear explosions. Although seismological capacity for identifying underground nuclear explosions may now be secondary to the political will of parties engaged in Comprehensive Test Ban negotiations, it is still important to present the clearest possible evaluation of the role seismology might play should a Comprehensive Test Ban become a reality.

One of the most important contributions to the improvement of world-wide

seismological resources was the establishment in the early 1960's of the World Wide Standard Seismograph Network (WWSSN). This network has been invaluable in establishing global seismicity patterns and has provided an excellent data source for seismological research on earth structure, in particular the seismological aspects of global tectonics. Although we shall demonstrate that the WWSSN has made and can make a contribution to seismological research on earthquake–explosion discrimination, the major portion of the special seismological funds and research effort in this field have been directed toward the installation and evaluation of special seismograph systems (arrays and improved single stations) which can reduce the seismic event detection threshold by signal enhancement relative to ambient noise levels. These special systems have, in turn, become exceedingly useful tools for general seismological research.

One of the principal factors contributing to the delay in international agreement on a treaty banning underground nuclear explosions has been the significant gap in explosion size between the general world-wide capacity for identifying seismic events, and the politically acceptable explosion size below which it might be assumed that little military advantage can be gained in successful clandestine testing. In an attempt to reach this lower level of identification, much of the emphasis is, of course, focused on the special seismograph systems referred to. In doing so, however, the seismologists concerned with nuclear explosion identification may have neglected an important step: the definition of the capacity of currently operational standard seismograph stations in regions of the world where relatively dense networks of these stations exist, by establishing discrimination techniques using known underground explosions and nearby earthquakes. These studies are severely restricted (in the world-wide context) to the areas of North America and the Soviet Union where explosions have been detonated by the two principal nuclear powers.

Data from numerous standard stations in North America, including stations close to the United States testing sites, have been extensively used for seismological discrimination research, principally by USA and Canadian seismologists. The existing capacity of standard stations for identifying underground explosions in USA is therefore much better defined than for USSR explosions. For example, Basham & Whitham (1971) used the results of Basham (1969a) to demonstrate that it is possible to identify underground explosions down to yields of 10–20 kt (all yields are quoted in terms of explosions fully contained in a hard rock environment) located within the USA using seismograms of standard stations in Canada. The results achieved by Evernden *et al.* (1971) suggest that by employing standard stations within the USA this threshold is significantly below 10 kt. Because of the lack of supporting data, it was difficult to extrapolate this result to explosions within the USSR.

The purpose of this paper is to present the results of an analysis of the capacity of standard (WWSSN) stations in Eurasia for identifying underground explosions in the USSR. The analysis relies heavily on the spectral differences between explosions and earthquakes as measured by $M_s : m_b$. Earlier studies have shown that considerable differences in the absolute levels of M_s result when Rayleigh waves propagate over different continental and mixed continental and oceanic paths, and when measurements are based on different properties of the Rayleigh wave train. To resolve these differences a complete re-evaluation of M_s is undertaken and an improved M_s scale is derived that accounts for the first order differences in path propagation effects; it also allows the remaining differences in path propagation effects; it also allows the remaining differences in $M_s : m_b$ relationships, particularly for explosions, to be interpreted more directly in terms of source phenomena. Second order path propagation effects on M_s remain, and these can only be accounted for as station corrections for particular source regions. The discrimination allowed by $M_s : m_b$ is further enhanced by applying a source depth correction to M_s, determined from the relative frequency content of the Rayleigh waves.

Employing the improved M_s formula, it is shown that M_s is a more stable measure of the 'size' of seismic events and yields for underground explosions, and a more useful magnitude scale than the previously employed m_b, for defining identification thresholds.

2. Stations, events and data

The map of Eurasia in Fig. 1 shows the locations of stations and events used in this study. The 90 earthquakes occurred in the five separate regions illustrated on the map and included all earthquakes with $m_b \geqslant 4{\cdot}0$ and $h \leqslant 50$ km located by the United States National Ocean Survey (NOS; formerly Coast and Geodetic Survey) for the year 1969. The earthquakes were restricted to these five regions because they are in close proximity to the known USSR underground explosions. Earthquakes in the active western Pacific seismic zones (Kamchatka, Kuriles, Japan, etc.) and south of the arbitrary southern boundaries of Regions I to IV were omitted in the selection of events.

To collect a suitable sample of explosions, we have employed all NOS-located explosions for 1968, 1969 and the first half of 1970 in the USSR. The 33 explosions occurred at eight different sites with the number of explosions at each of the sites shown adjacent to the site location in Fig. 1.

The 42 WWSSN stations whose records were employed are also shown in Fig. 1; these include all Eurasian (and off-shore) WWSSN stations that deposit seismograms

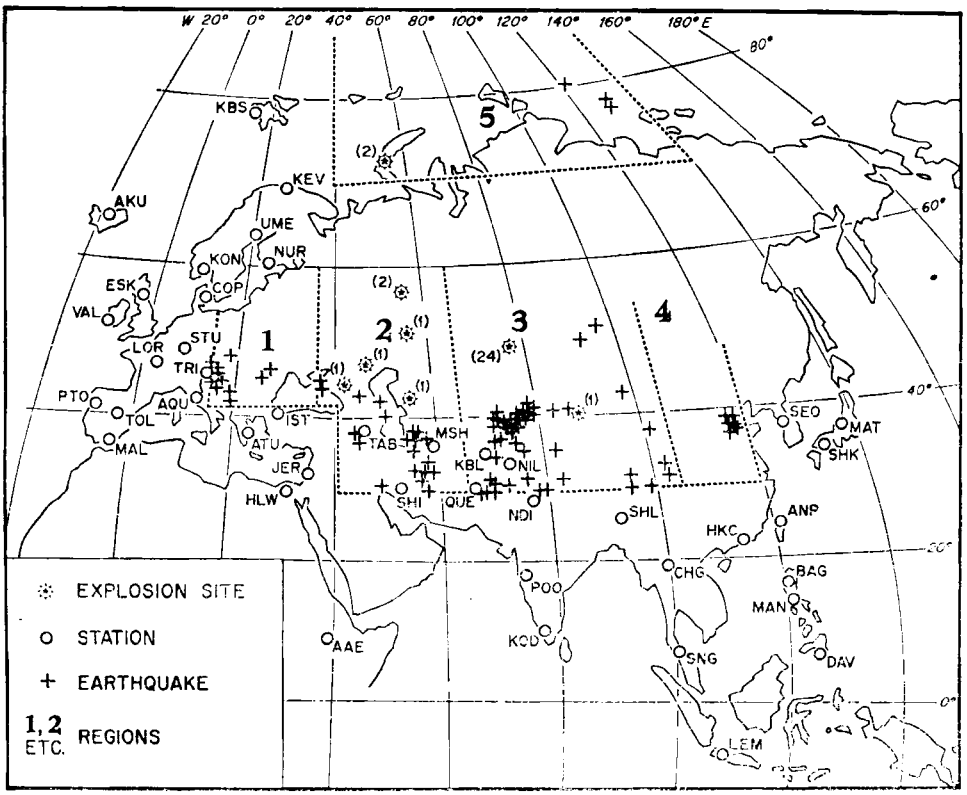

FIG. 1. Map of Eurasia showing the 42 WWSSN stations, the explosion test sites with bracketed number showing the number of explosions at each site, and the Eurasian earthquakes employed in this analysis. The broken lines illustrate the boundaries of the regions discussed separately for $M_s : m_b$ discrimination.

at the United States Seismological Data Center, from which microfilm copies were purchased for this analysis. In many instances stations were inoperative or had not deposited seismograms at the Data Center for various period of time required in this study and an average of 30 records per event were available from the 42 stations shown in Fig. 1. Although this is a rather serious problem from the point of view of the free exchange of seismological data, it did not detract significantly from this study because of the high quality and continuity of a number of key stations.

3. Rayleigh wave magnitudes (M_s)

3.1 *The magnitude scales*

The amplitude of surface waves were first used by Gutenberg (1945) to estimate the magnitude of a seismic disturbance:

$$M_s^G = \log_{10} A + B(\Delta)$$

where A is the amplitude of the resolved horizontal ground motion at a period of 20 s and $B(\Delta)$ is a distance normalizing term that corrects for the effects of geometric spreading, dispersion and absorption of the propagating surface wave. This formula was originally designed to use amplitude data from horizontal seismographs, but when vertical component systems came into general use, it was common practice to measure vertical displacements instead. The formula was developed empirically for events recorded at epicentral distances greater than 20°, and was based on the supposition that the maximum trace amplitudes correspond to waves with period of about 20 s.

The next important step in the development of the M_s scale can be attributed to Vanek *et al.* (1962) who proposed the formula

$$M_s^P = \log (A/T)_{max} + 1{\cdot}66 \log \Delta + 3.3.$$

This ' Prague formula ' employed a geographic average of various distance normalizing terms, and incorporated T in the formula to account for those cases, particularly for continental propagation and using broad band (Kirnos-type) seismographs, for which the maximum trace amplitude did not occur at a period near 20 s. In principle, the advantages of M_s^P are that it can be used over any epicentral distance range and the measurement is not restricted to a fixed period.

Data obtained at distances greater than about 25° give a value for M_s^P that is close to M_s^G, generally within 0·2 magnitude units. This is to be expected since Gutenberg's $B(\Delta)$ is in close agreement with the Prague term $1{\cdot}66 \log \Delta$, and the maximum amplitude at large distances frequently occurs around 20 s. However, M_s^P computed from close-in measurements at periods shorter than 20 s is usually larger than M_s^P computed from distant observations ($\Delta > 25°$) with periods near 20 s. For example, Basham (1969a) estimates the magnitude of Greeley, a Nevada underground explosion, as M_s^P 6·1 using regional data compared with a magnitude of M_s^G 5·1 estimated from long range observations.

Problems of this type have led to considerable confusion in published research related to identification of underground explosions on the basis of $M_s : m_b$, and particularly in relation to a comparison of small events observed only at near distances and larger events observed at greater distances. In pursuit of a solution to these problems of the application of existing M_s formulae to studies of underground explosion identification, the following sections give discussions of and suggested improvements to the M_s scale. The salient features of the distance corrections, the cause and effects of dominant surface wave periods, the effects of path propagation and the influence of focal depth are discussed separately to arrive at an improved M_s scale.

3.2 *The distance correction B′ (Δ)*

The $B(\Delta)$ distance correction term of Gutenberg (1945), an empirical relationship $1{\cdot}656 \log \Delta + 1{\cdot}818$, and the geographic average term adopted by Vanek *et al.* (1962), $1{\cdot}66 \log \Delta + 2{\cdot}0$ (for $T = 20$ s), both imply that the amplitude decrement with distance of 20-s waves due to geometric spreading, dispersion and absorption is proportional to $\Delta^{-5/3}$. The small difference in the constant terms gives rise to a small shift in the absolute levels ($M_s^P = M_s^G + 0{\cdot}2$) if the two formulae are applied to the same 20-s waves. All recent studies of M_s have shown that, when applied to 20-s waves for epicentral distances greater than about 25°, this distance correction will yield, to within the required accuracy, M_s values that are independent of distance, however dependent they may still be on source and path propagation effects.

Recent considerations of M_s^P at nearer distances in North America by Evernden (1971) and Basham (1971) have shown that for distances up to about 26° M_s^P increases with distance, the implication being that $1{\cdot}66 \log \Delta$ is not the appropriate correction for $\Delta < 25°$. Evernden's data, measured on Long Range Seismic Measurements (LRSM) long period narrow band seismograms, for earthquake Rayleigh waves at periods of 17–19 s and explosion Rayleigh waves at periods of 10–14 s suggest the appropriate distance correction to be $1{\cdot}0 \log \Delta$. Basham's data measured on wider band Canadian network long period seismograms for both earthquakes and explosions in the period range 8–14 s suggest the appropriate correction is $0{\cdot}8 \log \Delta$. The difference in the two studies between the dominant periods of earthquake maximum amplitude trace motion is related to the band of the recording system relative to the Rayleigh wave spectra, the LRSM pass band being more selective of the longer period portion of the earthquake spectrum, the broader band records showing maximum amplitudes at shorter periods for both source types. However, irrespective of the relative amplitudes of the Rayleigh components in this, say, 8– to 19–s range (the matter covered in Sections 3.3 and 3.4), these waves attenuate significantly less rapidly with distance than assumed using the $1{\cdot}66 \log \Delta$ correction.

Examination of group velocity curves for paths over North America shows a clear minimum centered near 12-s period. This means that for epicentral distances at which frequency-dependent absorption and scattering have not significantly affected this period range, the maximum amplitude in the Rayleigh wave train measured on a wider band seismogram to compute M_s^P will be an Airy phase with periods near 12 s. If so, the dispersion effects are nil, and the geometric spreading term is proportional to $\Delta^{-5/6}$ (Ewing, Press & Jardetzky 1957, p. 165. Brune 1962). If, for these shorter period waves, Q is taken as 1000, absorption will have little effect for small epicentral distances, and the appropriate M_s distance correction term will be $0{\cdot}8 \log \Delta$.

Beyond epicentral distances of 25°, the wave train generally becomes well dispersed, absorption effects become more important, and the effects of scattering and refraction on the Rayleigh waves become more apparent. The total of these results in a seismogram in which 20-s period energy is clearly visible and is often the maximum amplitude, so the magnitude measurements M_s^P and M_s^G are in fair agreement at epicentral distances greater than 25°.

We therefore propose that for distances up to 25° the distance dependence term, $B'(\Delta)$, be proportional to $0{\cdot}8 \log \Delta$, and at large teleseismic distances be the same as Gutenberg's $B(\Delta)$, which in turn is very close to $1{\cdot}66 \log \Delta$ used in the Prague formula. The $B'(\Delta)$ base line level in the range 0–25° is set so a smooth curve of $B'(\Delta)$ as a function of Δ is obtained. The absolute level of $B'(\Delta)$ is adjusted so that magnitude determinations from the new formula M_s will give results essentially the same as those when M_s^G or M_s^P are used on seismograms recorded at large epicentral distances. These values of $B'(\Delta)$ are tabulated in Table 1 and are appropriate to displacement defined in nm; i.e. $B'(\Delta)$ will be about 3·0 smaller than the distance corrections required for M_s^G or M_s^P based on displacement in microns.

Table 1

B′(Δ), *A revised distance correction function for* M_s

Δ°	B′	Δ°	B′	Δ°	B′	Δ°	B′	Δ°	B′
		20	1·25	40	1·57	60	1·85	80	2·08
1	0·17	21	1·27	41	1·59	61	1·87	81	2·09
2	0·35	22	1·29	42	1·61	62	1·89	82	2·10
3	0·57	23	1·31	43	1·62	63	1·90	83	2·11
4	0·67	24	1·32	44	1·64	64	1·91	84	2·12
5	0·78	25	1·34	45	1·65	65	1·92	85	2·13
6	0·84	26	1·36	46	1·66	66	1·93	86	2·14
7	0·90	27	1·38	47	1·68	67	1·94	87	2·15
8	0·95	28	1·40	48	1·70	68	1·95	88	2·16
9	0·98	29	1·41	49	1·71	69	1·96	89	2·17
10	1·02	30	1·43	50	1·72	70	1·97	90	2·18
11	1·05	31	1·44	51	1·74	71	1·98	91	2·18
12	1·08	32	1·45	52	1·75	72	1·99	92	2·19
13	1·11	33	1·47	53	1·76	73	2·01	93	2·20
14	1·13	34	1·48	54	1·77	74	2·02	94	2·21
15	1·15	35	1·50	55	1·78	75	2·03	95	2·22
16	1·17	36	1·52	56	1·80	76	2·04	96	2·23
17	1·19	37	1·54	57	1·82	77	2·05	97	2·24
18	1·21	38	1·55	58	1·83	78	2·06	98	2·25
19	1·23	39	1·56	59	1·84	79	2·07	99	2·26

3.3 *Rayleigh wave period considerations*

The amplitude near 20-s period is measured to estimate M_s^G and period has no further significance. For M_s^P, however, T is a significant term. Given a flat spectrum, in which all periods have the same amplitude, it is easily seen that as T gets shorter M_s^P gets larger. Taking Greely as an example, it has already been shown that where absorption has not removed the shorter period energy, the M_s^P magnitude is relatively larger than at great distances where $(A/T)_{max}$ is measured at a longer period. Part of this difference is due to T in the formula, and part is due to the relatively larger amplitude at the shorter periods. This introduces the whole question of why the maximum Rayleigh ground motion amplitude occurs at a particular period, and how to measure the seismogram amplitudes to compute an M_s value that is accurate relative to some absolute base.

We will initially confine considerations to the passband of the WWSSN long period seismograph (approximately constant in magnification from about 10 to 30 s) which allows us to see much more of the source-dependent effects than a narrower band instrument. Note that for a narrow band instrument, such as the LRSM instrument, the period of observed maximum amplitude becomes more dependent on the exact passband and is less representative of true maximum ground motion. In addition, it is obvious from detection threshold considerations that one should employ the largest amplitude on the seismogram; for the records employed here, this is generally within the 10- to 30-s range, but under special circumstances (e.g. very near distances) the maximum amplitudes may occur at shorter periods.

The period of the wave with maximum ground motion depends on the initial spectral distribution of energy by the source, the source depth, the dispersion characteristics of the transmission path over which the wave propagates, and the absorption properties of the path. How each of these phenomena contribute to the seismogram can be discussed separately; but we need to do so only in general terms: recall that we are dealing with magnitudes (logarithms of amplitudes) and perturbations of the order of 20–30 per cent will not be significant. In the context of earthquake–explosion

discrimination, it is the significant difference in spectral distribution at high and low frequencies that is employed in the $M_s : m_b$ criterion.

The completely arbitrary but historically accepted absolute base of M_s is the estimated size of the 20-s source component. We retain this base in the sense that the distance correction (Section 3.2) is normalized to the Gutenberg value at large distances, and the path correction (next section) is relative to the value at 20 s. But, however accurately we may correct for the source depth and propagation path, the general character of the wide band seismogram must depend significantly on the initial spectral distribution by the source. For any general population of events for which M_s values are to be computed, there is no *a priori* knowledge of the source spectrum, and thus no means of correcting for relative differences among events between the measured maximum amplitude and the 20-s amplitude due solely to the source. The only means of avoiding this problem is to redefine the magnitude in terms of an estimate of total energy released by an event, a suggestion that has been made often, but which remains impractical for general application. However, a magnitude defined on the basis of the maximum Rayleigh wave amplitude is a more consistent measure of the relative sizes of seismic sources.

The effects of source depth on the surface wave amplitudes involve the nature and orientation of the source, and the Earth's structure in the vicinity of the source, but in general the deeper the source the less short period energy is observed in the surface wave train. A Rayleigh wave spectrum frequently contains a minimum which may be related to the exact nature of the source, its depth and the structure in the vicinity of the source (see, for example, Tsai & Aki 1970). If this spectral minimum occurs at a period that would have appeared as a maximum amplitude for events at some other depth, then we encounter a further unknown effect that can be considered part of the general problem of spectral distribution by the source discussed above. However, the general phenomenon of the reduction of shorter period Rayleigh wave energy with increasing focal depth can be treated by a correction to M_s, and is discussed in Section 3.5.

The dispersion characteristics of a particular path have a considerable effect of shaping the amplitude envelope of the surface wave train. For example, a minimum in the group velocity curve for a continental path causes a number of periods to arrive at a recording station at about the same time, resulting in an Airy phase, a large pulse-like arrival on the seismogram. Waves from the same event recorded over a path with thick sedimentary layers suffer dispersion of the shorter period waves, which are confined to the upper sedimentary layers. The result is that waves with different periods travel with different group velocities, are spread out in time and no pulse-like arrival is read. When the amplitude measured is that of an Airy phase, the M_s value will be large compared with the value determined from a surface wave train without an Airy phase.

The dispersion effects as a function of distance, i.e. greater dispersion and thus smaller amplitudes for fixed period waves at greater distances, are accounted for along with geometric spreading and absorption by the distance correction term (Section 3.2). For a magnitude scale based on the maximum amplitude on the seismogram, we require corrections for the relative differences in dispersion effects among the different period waves as a function of the propagation path. These are described in the following section.

3.4 *The path correction*

The approximate amplitude envelope of a surface wave train may be predicted using the method of stationary phase (Ewing *et al.* 1957). By rearranging and substituting a few terms, Carpenter & Marshall (1970) showed that an expression involving readily evaluated terms can be derived to define the amplitude envelopes due to the dispersive characteristics of the path. This envelope is determined by evaluating

the expression $UT^{-3/2}(dU/dT)^{-1/2}$, where U is the group velocity, T the period and dU/dT the slope of the group velocity-period curve.

The primary study reported here is the application of $M_s : m_b$ discrimination to Eurasian earthquakes and explosions, and the initial requirement and test case for a path correction was for application to Rayleigh waves that traverse various paths in different directions across the Eurasian continent. To examine the variations in, and establish an average for, the amplitude envelope for Eurasian propagation, we analysed 30 group velocity curves, some from published papers and some from our analysis of Rayleigh wave trains. The stationary phase estimate was made where possible in the period range 10- to 60-s at 5-s intervals. The estimates at each of the period values were averaged to produce an amplitude envelope as a function of period that was representative of the average transmission path in Eurasia. This amplitude envelope in arbitrary (cgs) units is shown in Fig. 2 with standard deviation bars of the stationary phase estimates.

For purposes of comparing the Eurasian path effects to those in other areas and in order to remove path effects to compare events in North America and Eurasia, three additional amplitude envelopes were determined: one an average for continental North American propagation (derived from four group velocity curves), one for intercontinental propagation (from central Asia to central Canada), and one for oceanic propagation (from the Aleutian Islands to the west coast of the United States); the two latter envelopes were derived from single group velocity curves. These are the three additional amplitude envelopes shown in Fig. 2.

These curves show that for an impulsive input into the North American path, the amplitude at 10-s period is about seven times larger than the amplitude at 20 s, due to the dispersion characteristics of the path alone; over an Eurasian path the amplitude difference between 10 and 20 s is only a factor of two. The predicted amplitude at 20-s period for both paths is, however, almost equal, which means that, if the same source was situated in both Eurasia and North America and recorded over a continental path, they would give the same magnitude if the amplitudes were measured at 20-s period. Both the oceanic and intercontinental paths exhibit relatively low amplitudes at the shorter periods, the oceanic path being slightly above and the intercontinental path slightly below the continental paths at 20 s. It is therefore clear why, if the amplitude data is measured at periods shorter than 20 s, large differences will occur in the M_s^P value for events of the same size over different paths.

All that remains is to convert the amplitude envelopes into path corrections that are a function of period relative to the amplitude of 20 s. The amplitude predictions for Eurasian and North American paths are almost the same at 20 s, so this is used as the zero base for the path corrections. For convenience and ease of programming, straight lines were fitted through the amplitude envelopes from 10- to 20-s period, and from 20 to 40 seconds and to a magnitude correction. The four separate path corrections for magnitude are shown in Table 2. For all paths the results are similar near 20-s period, confirming Guthenberg's M_s^G as a good average surface wave magnitude over any path.

The proposed M_s scale can now be written as

$$M_s = \log A + B'(\Delta) + P(T)$$

where A is the maximum amplitude (nm) in the Rayleigh wave train, $B'(\Delta)$ is given in Table 1 and $P(T)$ is the path correction (Table 2) varying with the period of the wave measured and the particular path as derived above. To summarize this derivation M_s enables us to use the maximum Rayleigh wave amplitude on the seismogram; this is an obvious advantage for small events where only one or two cycles remain above the microseismic noise. The period at which the maximum amplitude occurs is determined for shallow seismic sources primarily by the dispersive characteristics of the path, for which a correction has been evaluated. The distance dependence term

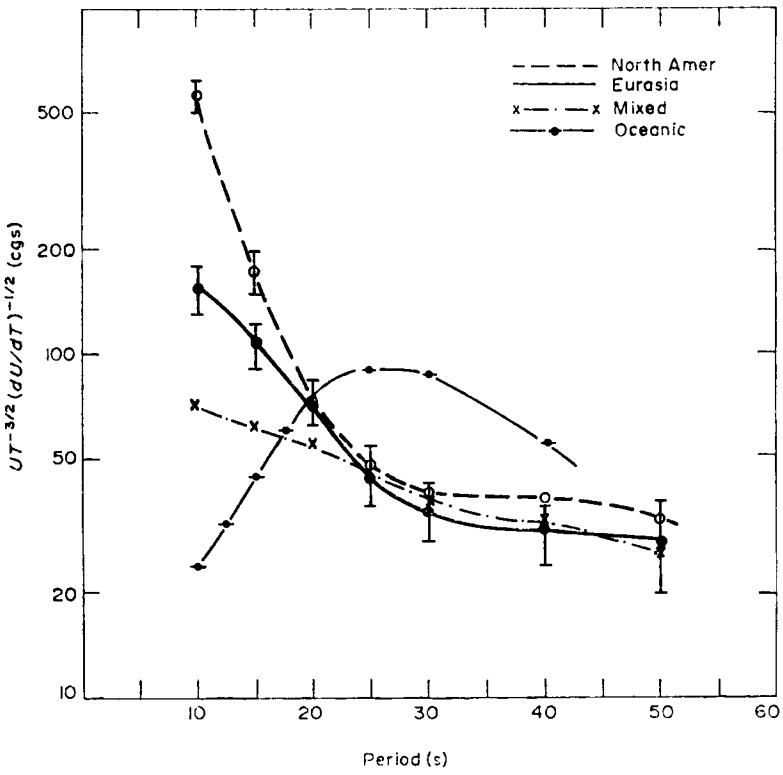

FIG. 2. Amplitude envelopes of vertical component Rayleigh waves as a function of period determined by the stationary phase approximation from the group velocity (U) versus period (T) curves for four transmission paths. The Eurasian and North American continental curves are the means of 30 and four determinations, respectively; standard deviation bars at each period are shown. The remaining two curves are examples for the particular transmission paths.

assumes that over short continental transmission paths the largest amplitude is in the Airy phase that decays as $\Delta^{-5/6}$. Since most seismic events recorded at short distances are propagated over continental paths, and most seismic recording stations are on continents, this determination of M_s should be more accurate with what we believe to be a more precise distance dependence term. The absolute level of B' (Δ) has been set such that M_s determinations made with the formula proposed here agree within $\pm \cdot 1$ of a magnitude unit with Gutenberg's formula and the Prague formula when 20-s period amplitude data are used from seismograms recorded at distances greater than 25°.

Before evaluating the proposed magnitude M_s, the one remaining effect referred to in Section 3.3 (the effect the depth has on the surface waves) is to be discussed. This is a rather important effect when considering the differences between explosions and earthquakes and is treated in detail in the next section.

3.5 *Rayleigh wave spectral content and focal depth corrections*

The research presented in this paper is oriented toward discrimination between explosions and earthquakes by analysis of seismic data, and the improvements to the M_s scale discussed above are designed to standardize the heretofore variable base of the M_s scale when employing the relative enrichment of explosion short period energy (as measured by m_b) to discriminate the explosions from the earthquakes. However,

Table 2

Magnitude corrections for selected paths as a function of period, P(T)

		M_s Correction		
T (s)	Continental N. America	Continental Eurasia	Mixed Cont.–Oc.	Oceanic
10	−0·75	−0·30	+0·00	+0·50
11	−0·67	−0·27	+0·01	+0·45
12	−0·61	−0·24	+0·03	+0·38
13	−0·53	−0·21	+0·04	+0·33
14	−0·46	−0·18	+0·05	+0·27
15	−0·38	−0·15	+0·07	+0·20
16	−0·30	−0·13	+0·08	+0·15
17	−0·24	−0·10	+0·09	+0·09
18	−0·16	−0·07	+0·10	+0·03
19	−0·08	−0·04	+0·12	−0·03
20	+0·00	+0·00	+0·13	−0·09
21	+0·01	+0·03	+0·15	−0·08
22	+0·03	+0·05	+0·16	−0·07
23	+0·04	+0·07	+0·17	−0·06
24	+0·05	+0·11	+0·18	−0·05
25	+0·07	+0·14	+0·20	−0·04
26	+0·09	+0·18	+0·21	−0·03
27	+0·11	+0·22	+0·22	−0·03
28	+0·13	+0·24	+0·23	−0·02
29	+0·14	+0·27	+0·24	−0·01
30	+0·16	+0·30	+0·25	+0·00
31	+0·17	+0·32	+0·26	+0·01
32	+0·18	+0·33	+0·27	+0·02
33	+0·20	+0·34	+0·28	+0·03
34	+0·21	+0·35	+0·29	+0·04
35	+0·23	+0·36	+0·30	+0·05
36	+0·25	+0·37	+0·31	+0·06
37	+0·27	+0·38	+0·32	+0·07
38	+0·28	+0·39	+0·33	+0·08
39	+0·29	+0·40	+0·34	+0·09
40	+0·31	+0·41	+0·35	+0·10

it has often been stated that a large majority of earthquakes could be disregarded in discrimination studies if the focal depths of events could be established to within about ±5 km. This is unachievable at present and is likely to remain so for some time; one recent estimate has suggested, however, that employing available seismic records with the specific intent of identifying depth phases (*pP*, *sP*, *pPcP*, etc.) could eliminate about 50 per cent of all earthquakes from consideration as possible explosions. It is the supposition that all focal depths greater than about 50 km are, within the errors of hypocentre location, sufficiently deep to preclude the possibility of the event being an underground explosion that allows these events to be ignored in discrimination studies. This supposition is employed in selecting only events shallower than 50 km for this discrimination study. In the absence of special studies to define accurate depths for some of the shallower events, it is prudent to include all of them in discrimination studies. We will show, however, that Rayleigh wave frequency content is sufficiently variable, for source depths of 0–50±25 km, that it can be used to advantage in discrimination studies.

It must, however, be stressed that the following does not include a technique to identify the depth of focus of a source; it simply makes use of the intrinsic spectral differences between explosion—and earthquake—generated Rayleigh waves to assist discrimination between the two types of sources.

Consider briefly the effect source depth has on the Rayleigh wave spectrum

observed at the surface. As the focus of a seismic event gets deeper, the Rayleigh wave train generated and observed on the surface at a distance becomes progressively less rich in high frequency energy, i.e. the observed spectrum peaks at a progressively lower frequency. Coupled with this effect of focal depth will be the spectral distribution by the source itself; the two effects cannot be easily isolated. The source depth of explosions varies only over a few kilometres and these effects would appear only in the shortest Rayleigh wave periods, near 6-s period, which is the middle of the Earth microseismic noise band. These Rayleigh waves are rapidly attenuated with distance and, since the response of the standard recording instrument is falling off at these periods in order to attenuate the microseisms, they are not observed other than very close to the source. The effects of focal depth on observed Rayleigh waves from earthquakes, which may occur at appreciable depths, should however be apparent within the standard seismograph passband.

To see how sensitive this effect might be, we measured Rayleigh wave amplitudes for the Eurasian events (earthquakes and explosions) at (*a*) the shortest period clearly observable, (*b*) the period closest to 20 s and (*c*) the longest period clearly observable, and calculated M_s^P for each. For each event average magnitudes were determined from available measurements in the three period ranges, $T < 17$ s, $17 \leqslant T \leqslant 23$ s and $T > 23$ s, and were designated M_1, M_2 and M_3, respectively. Values of M_1, M_2 and M_3 were plotted as $(M_1 - M_2)$ and $(M_1 - M_3)$ against available computed NOS depths (i.e. ignoring events with $h = 33$ or N) and a least squares line drawn through each group. This calibration of our event-station network in terms of magnitudes and depths was then used to estimate new depths for all events: i.e. after employing the NOS depths to define the calibration lines, the NOS depths were discarded. The actual relationships derived and employed were $h(\text{km}) = 38 - 47$ $(M_1 - M_2)$ and $h(\text{km}) = 51 - 41$ $(M_1 - M_3)$. The final Rayleigh wave estimate of depth adopted was the average of these two estimates if both were available, a single estimate if only one was available, or $h = 0$ if the Rayleigh magnitude was available in only one of the period ranges. A third depth estimate in terms of $(M_2 - M_3)$ could have been made, but the two chosen were in sufficiently good agreement to make it unnecessary.

The number of events assigned focal depths by this procedure in each 10 km depth interval and the number of events for which no determination could be made are shown in Table 3. The absence of a depth estimate (i.e. setting $h = 0$) is the worst situation in terms of discrimination because the event must be assumed to have a surface focus and no M_s correction can be applied to account for the fact that the event may be at considerable depth. The latter is usually the situation for the small events with one or two Rayleigh wave cycles observed above the noise.

The ability to determine these Rayleigh wave depths and M_s depth corrections depends to a great extent on the size of the recorded Rayleigh waves; it is possible for a majority of the earthquakes, but less than half of the explosions, because most of the earthquakes have M_s values in the range 4·0 to 5·0, whereas most of the explosions have M_s values in the range 3·0 to 4·0 (see, for example, Fig. 7). With the Rayleigh wave period content calibrated against NOS computed depths, a similar range of

Table 3

Focal depths and M_s depth corrections assigned from Rayleigh wave measurements

Depth range (km)	0–9	10–19	20–29	30–39	40–49	50–59	60–78	No determination ($h = 0$)
No. explosions	6	4	2	1	0	0	0	17
No. earthquakes	2	15	34	16	6	3	3	4
Mean depth correction	0·04	0·12	0·20	0·28	0·36	0·44	0·56	0·00

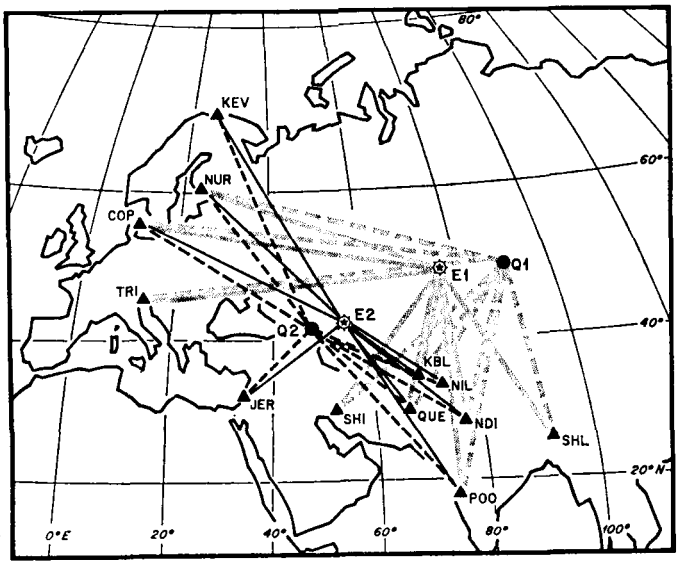

FIG. 3. Base map showing approximate paths from events to the stations for the Rayleigh waves illustrated in Figs 4 and 5. Pertinent information on the two explosions (E1, E2) and the two earthquakes (Q1, Q2) is given in Table 3.

depths will result, but the procedure when applied in this unbiased manner does place a majority of the earthquakes in the depth range 10 to 40 km and indicates depths of less than 10 km for about half of the explosions to which it can be applied. The Rayleigh wave depths and consequent depth corrections do become unreliable, as indicated by explosions assigned depths of 20 or 30 km, when the required Rayleigh wave spectral content can be observed at only one or two stations; in this case the observed Rayleigh wave content can be heavily dependent on the particular path, a dependence which tends to be averaged out if the appropriate measurements can be made at a large number of stations.

This procedure is admittedly imperfect and perhaps has limited seismological value, but it does make effective use of discriminatory information directly measurable on the seismograms. The M_s focal depth correction applied is Bath's (1952) additive term $0{\cdot}008h$ where h is the depth in km; this effectively normalizes M_s to the equivalent value for a surface focus event. The value of the depth correction in assisting to discriminate explosions and earthquakes is subsequently demonstrated, but the average effect can be seen in Table 3: for the events employed here the earthquake M_s values are increased on the average by about 0·2 whereas explosion M_s values, with the exception of those few explosions assigned improbable depths, are relatively unaffected. In this evaluation of the $M_s : m_b$ criteria, an identical procedure is applied to all events, but any large depth correction assigned to an identified explosion should be removed in order to obtain the best estimate of M_s for that explosion; this is done here for all such explosions following their identification on the $M_s : m_b$ plots.

To summarize the M_s computation: the M_s value of each event was determined from the maximum ground displacement, corrected for distance and path effects at each station and averaged. The average M_s was then corrected for source depth using the estimated Rayleigh wave depth described above. Thus, the completed calculation

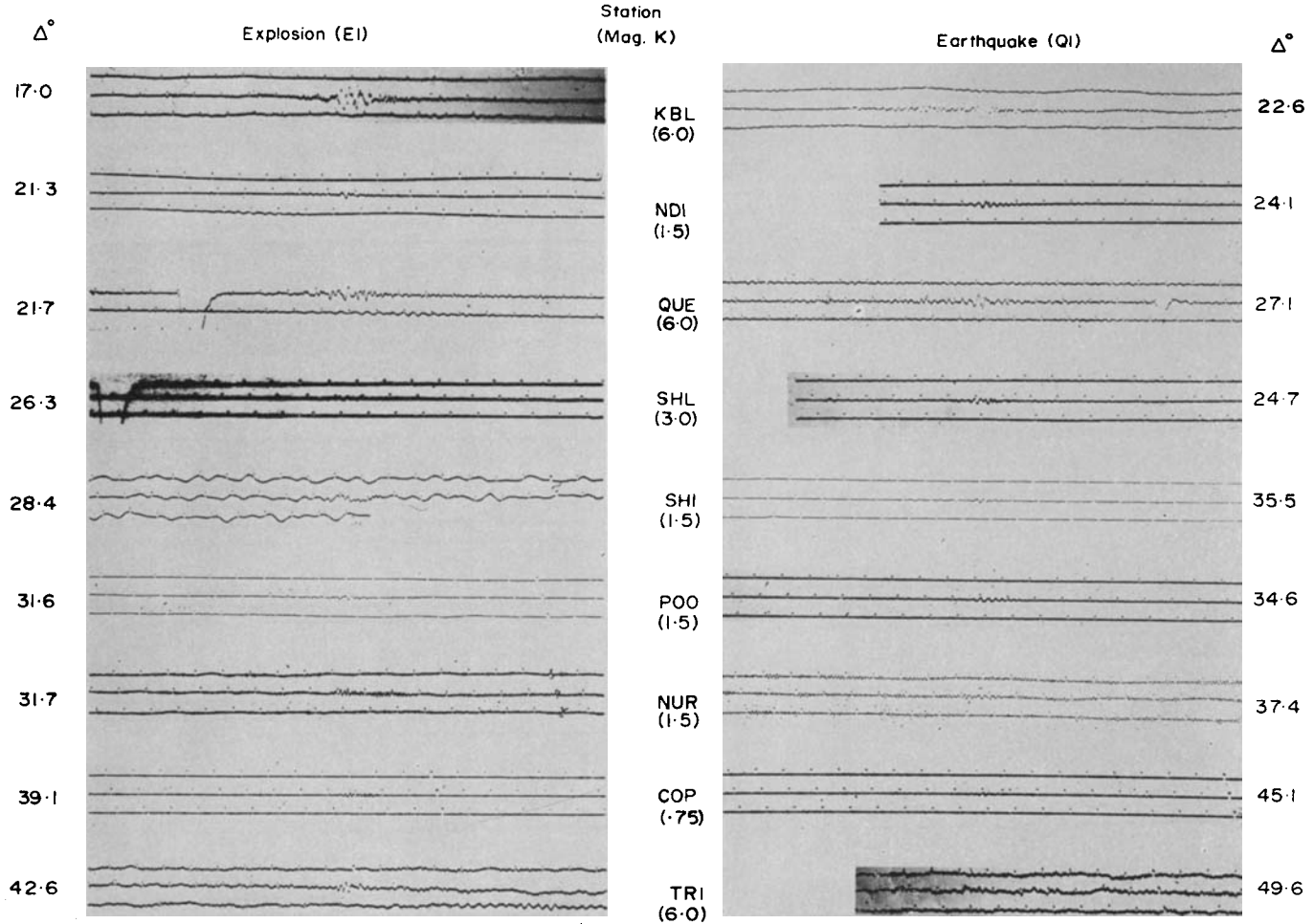

Facing p. 442

FIG. 4. Reproductions of vertical long-period seismograms from nine stations for explosion E1 and earthquake Q1 (see also Fig. 3 and Table 3). Rayleigh wave appears at the centre of the middle trace on each seismogram section, and records are aligned approximately on the largest amplitude motion. Records are reproduced from 35 mm positive microfilm and considerable loss of resolution is unavoidable.

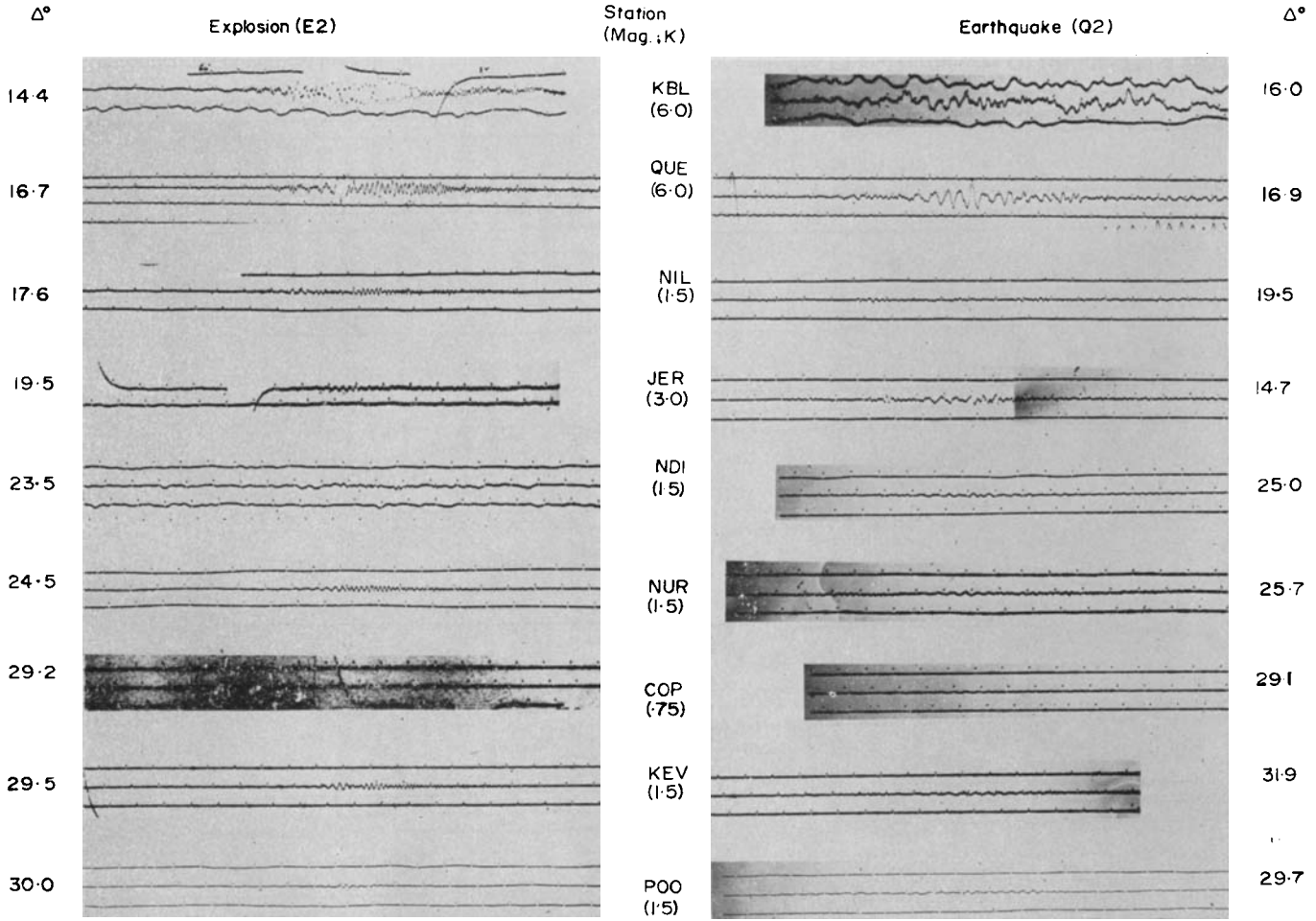

FIG. 5. As in Fig. 4 for explosion E2 and earthquake Q2. The COP record for E2 was badly fogged and could not be reproduced adequately, although Rayleigh wave is clearly visible on the microfilm.

can be written as

$$M_s \text{ (station)} = \log A_{\max} + B'(\Delta) + P(T)$$

$$M_s \text{ (final)} = M_s + 0{\cdot}008h.$$

One further note on the final M_s values is required. It is important to avoid the introduction of station bias into M_s values of events recorded at a small number of stations. Such biases can be described as second order path effects in the sense that any particular event-station path may be different from the average Eurasian path, which is accounted for by the path correction, $P(T)$. To eliminate this effect as much as possible, all events whose Rayleigh waves were recorded at fewer than five stations were considered for the application of station corrections (i.e. second order path corrections). This was done by determining, and applying where necessary, station corrections for the poorly recorded events on the basis of the particular station's response to larger, more widely recorded events from the test site or earthquake region in question.

3·6 *Rayleigh wave illustrations*

To illustrate some of the features of the explosion and earthquake Rayleigh waves noted in previous sections and to show the general signal and record quality available for the stations employed, seismogram reproductions are shown in Figs 4 and 5 for the four events and 12 stations illustrated on the base map in Fig. 3. The pertinent information on the four events is given in Table 4. Numerous features of the Rayleigh waves are apparent in these sample records, but only a few will be noted here. Note first that the two earthquakes and the two explosions have very similar magnitudes, the two earthquakes being about 0·9 smaller than the two explosions in m_b, and the explosions being about 0·3 smaller than the earthquakes in M_s (see Table 4). Note also that the Rayleigh waves for each of the four events were detected and measured at 21 to 23 stations; nine records for each event are reproduced in Figs 4 and 5.

Some path effects on the Rayleigh waves can be observed; for example, NDI, which is at a very similar epicentral distance for the two explosions and the two earthquakes, shows a pulse-like arrival of 2 to 3 cycles for E1 and Q1 in Fig. 4, but a more spread-out (but not obviously dispersed) arrival of energy for E2 and Q2 in Fig. 5. The two explosion records at KBL illustrate a striking variation in the path as it affects the high frequency Rayleigh wave propagation. Assuming an equivalent source spectrum for the two explosions and no large effect of the slightly greater distance for E1, the path for E2 is seen to be much more efficient in the propagation of the shorter period (sedimentary) Rayleigh waves. This effect is apparent to a lesser degree for the explosions at QUE.

The differences among the records in Figs 4 and 5 result from a combination of source spectrum, focal depth and path propagation effects and in many cases it is

Table 4

Data on events illustrated in Figs 4 *and* 5

	E1	Q1	E2	Q2
Region	E. Kazakh	Mongol.–USSR	W. Kazakh	Caspian
Co-ordinates:	49·9 N 79·0 E	50·3 N 91·2 E	43·8 N 54·7 E	40·2 N 50·2 E
Date:	1969 Nov. 30	1969 April 6	1969 Dec. 6	1969 Nov. 4
Time:	03:32:57·2	19:22:39·4	07:02:57·4	20:17:47·7
h (NOS):	(0)	31	(0)	29
h (from Rayleigh):	3	28	8	35
m_b:	5·98	4·78	5·84	4·85
M_s:	4·08	4·43	4·08	4·39
n (for M_s):	23	21	22	23

difficult to isolate the individual contributions of each effect. For example, Q2 with a similar, but slightly longer, path to KBL and QUE (than E2) has very little short period Rayleigh energy at these stations; this is most likely the result of both the smaller source excitation by the earthquake at the shorter periods and the effect of the much greater focal depth of the earthquake, with a possible contribution from the longer and slightly different path of the earthquake. The two earthquakes show in total among the records a significantly longer dominant period than the two explosions; assuming for the total suite of records the average path effect is similar for the earthquakes and explosions, this is due strictly to source excitation and focal depth effects.

By looking at the complete sets of records for the two earthquakes, the Rayleigh wave period content that is employed to determine the depth and the depth correction for M_s (Section 3.5) can be observed. On all records Q2, which has been assigned a Rayleigh wave depth of 35 km, has a much greater long period energy content than Q1, assigned a Rayleigh wave depth of 28 km. It can be noted that not all of this difference must necessarily be attributed to the effect of focal depth; the two earthquakes in two possibly quite different tectonic environments could have significantly different source spectra.

In one sense the above statements concerning these Rayleigh wave examples suggest a qualification on the statements made in Section 3.5 attributing the major variations in Rayleigh spectral content to focal depth. It may be more accurate to state that we are making an *ad hoc* correction to increase earthquake M_s values because it is generally observed that earthquakes tend to have longer period Rayleigh waves. However, for the 10- to 30-s band of the standard long period seismographs and for the distance range of about 15 to 45° employed here, we believe the focal depth to be a major influence and will retain the term 'depth correction'.

4. *P*-wave magnitudes (m_b)

The improved M_s scale that will be employed for discussions of discrimination in the following sections has been adjusted in details of the computational procedure, but retains the same basic absolute base as previous scales, the reasons for the modification having been explained in the previous section. No similar modifications have been attempted here for the m_b scale, although this is an important subject for extensive further research. The effect of this will, therefore, be, assuming the aims of the standardization of M_s have been achieved, to isolate existing relative discrepancies in m_b among events from different regions. In addition, such discrepancies that may exist are very easily observed on the principal diagrammatic scheme employed for discrimination, the $M_s : m_b$ plot.

Thus, the m_b values adopted for the Eurasian events studied are standard published (NOS) values, modified slightly to remove any obvious relative errors. The mean m_b values were recalculated from the NOS Earthquake Data Reports after removing all contributed values for epicentral distances less than 20°, the regional ($\Delta < 20°$) m_b values having been shown in numerous recent reports to be generally inconsistent with teleseismic determinations. Finally, all events for which P waves were observed at small numbers of stations were rechecked with respect to the requirement for station corrections in a manner similar to that described for M_s at the end of Section 3.5.

5. Re-evaluation of North American magnitudes

Before turning to the Eurasian events, which are our main concern, we illustrate the effect of improved M_s estimates by comparing reworked North American events with earlier studies. Most previous Canadian $M_s : m_b$ studies have used the Prague

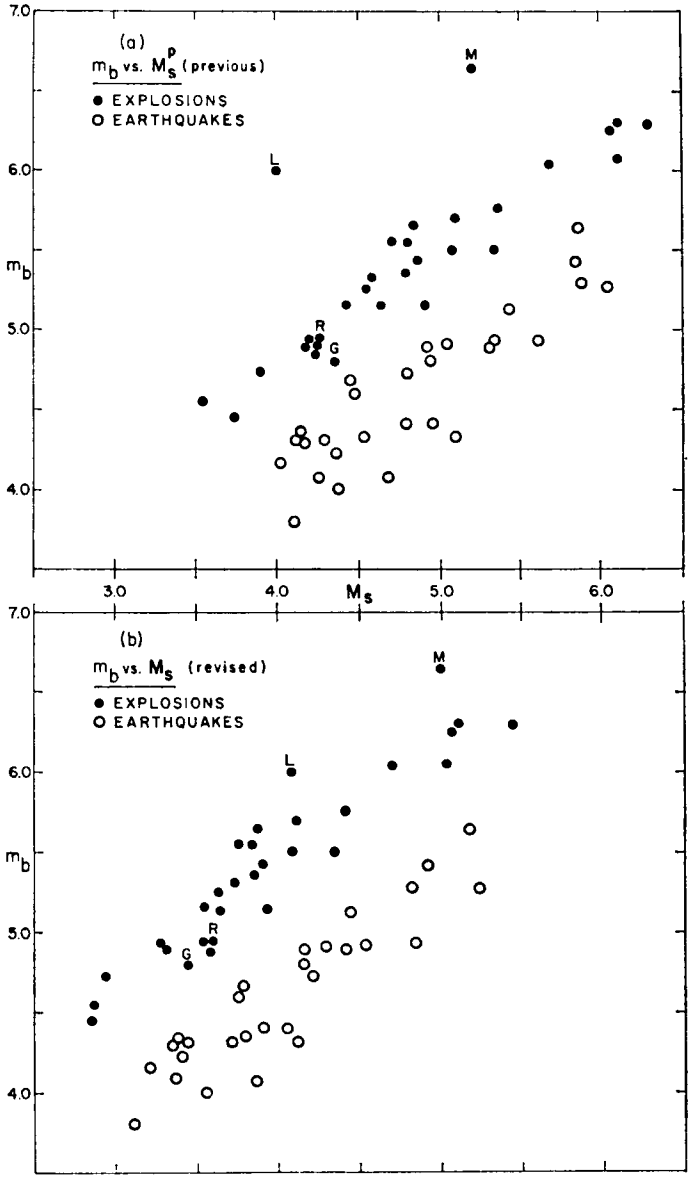

FIG. 6. $M_s : m_b$ plot of North American explosions and earthquakes: (a) upper diagram using the Prague M_s^P formula and (b) lower diagram using the revised M_s formula. The letters, L, M, R and G, denote the explosions Long Shot and Milrow (Aleutians), Rulison (Colorado) and Gasbuggy (New Mexico), respectively.

M_s^P formula for calculations of M_s, and these data are summarized in Fig. 6(*a*). The Aleutian Long Shot data are from the Canadian portion of the data of Lambert *et al.* (1969) and the Milrow data from the Canadian portion of the data collected by Liebermann & Basham (1971). The Colorado 'Plowshare' explosion, Rulison, magnitudes are from Basham & Halliday (1970) and Nevada Test Site (NTS) explosion, Benham, from Basham, Weichert & Anglin (1970). The New Mexico 'Plowshare' explosion, Gasbuggy, the remaining NTS explosions and the south-western North American earthquakes are from Basham (1969a).

The same events reworked to give M_s, but without the depth corrections (the original seismograms were not remeasured to establish the Rayleigh wave depths), are shown in Fig. 6(*b*). The source-to-Canada paths for Long Shot and Milrow are mixed and Rayleigh waves from the two explosions were recorded in Canada with periods near 20 s, near the common point of the magnitude scales (see Fig. 2 and Table 2); the M_s values are not changed significantly from M_s^P. However, the other explosions and earthquakes have continental paths to Canada and the Rayleigh waves are recorded with periods generally between 8 and 14 s. The effect of the path corrections is to reduce M_s relative to M_s^P. Though Long Shot and Milrow are now much closer to the main population of continental USA explosions, they are still sufficiently removed to warrant further discussion in a later section. Path corrections have also reduced the scatter in the earthquake population and thereby improved the separation between the two populations.

This is an appropriate point at which to discuss two alternative procedures for computing earthquake and explosion M_s values for purposes of discrimination. The first is that of Liebermann & Pomeroy (1969) who, for studies of NTS explosions and nearby earthquakes, employed the Gutenberg M_s^G formula and restricted their Rayleigh wave measurements to periods near 20 s. The discrimination (i.e. the separation between the two populations in $M_s : m_b$) may be improved by this procedure because it takes advantage of larger relative differences in source excitation near 20-s period than at shorter periods. Unfortunately, for visual seismograms, and particularly for continental Rayleigh waves, there can be a serious increase in the Rayleigh wave detection threshold if magnitudes are restricted to 20-s waves, an increase that can be equated to the North American path correction (with opposite sign) for periods shorter than 20 s, given in Table 2. The second procedure is one employed by Marshall for Eurasian events reported in the SIPRI (1968) report. The shorter period M_s values for small events observed at near distances were adjusted to yield equivalent 20-s magnitudes by calibrating the amplitudes of the shorter periods relative to 20 s generated by large control events.

The present method of computing M_s is an improvement on both of the above methods because equivalent 20-s magnitudes are obtained using the path corrections from maximum amplitude Rayleigh waves measured at any period within the long period seismograph passband. Thus, having confirmed the improvements achieved with the improved M_s for North American events, the next step is to apply the methods to the sample of Eurasian events described in Section 2. The North American data in Fig. 6(*b*) will be compared to the Eurasian data later in the paper.

6. Eurasian discrimination

6.1 *The regional data*

A summary of the Eurasian events for which Rayleigh waves were recorded is given in Table 5. The table lists the number of earthquakes and explosions in each region illustrated in Fig. 1, the number of Rayleigh waves partially and totally obscured by Rayleigh waves from other events, the number of explosions for which no Rayleigh waves were observed (Rayleigh waves were observed for all unobscured earthquakes) and the number of events for which M_s has been computed. No under-

Table 5

*Summary of event Rayleigh wave detections**

Region (see Fig. 1)	No. Earthquakes				No. Explosions				
	N	*P*	*O*	M_s	*N*	*P*	*O*	*ND*	M_s
I	11	1	1	10	0				
II	21	2	0	21	6	2	0	0	6
III	49	5	5	44	25	3	1	2	22
IV	6	0	1	5	0				
V	3	0	0	3	2	0	0	0	2
TOTAL	90	8	7	83	33	5	1	2	30

N: total number of events for the region

P: number of events with Rayleigh waves obscured by an interfering event over part of the network

O: number of events with Rayleigh waves obscured at all stations of the network

ND: number of events with no observable Rayleigh waves at the available network stations

M_s: number of events with M_s calculated

* Tables of events and final magnitudes are not included in this paper; these are available upon request to the authors.

ground explosions are known to have occurred in Regions I and IV, but the earthquakes for these two regions were included in order to evaluate discrimination with respect to the more-or-less continuous zone of earthquakes throughout Eurasia.

The data for events in the three regions containing known explosion test sites (Regions II; III and V) are shown in Fig. 7. Region V (see Fig. 1 and Fig. 7(*a*)), the Asian Arctic coast, is relatively aseismic, and the three Laptev Sea earthquakes selected for comparison with the two Novaya Zemlya explosions occurred at some distance from the explosion site. Although the data for Region V are too scarce to define trends, they do exhibit a distinct $M_s : m_b$ separation between explosions and earthquakes. Previous studies of Novaya Zemlya explosions (for example by Liebermann & Pomeroy (1969) and Basham (1969b)) compared the explosions to a larger suite of general Eurasian earthquakes; we are attempting here to compare events in a more restricted regional sense.

Fig. 7(*b*) compares 21 explosions from the eastern Kazakh test site and the one Sinkiang underground explosion, 'C', with 44 earthquakes in the general region of Tadzhik–Kirgiz–Sinkiang. Rayleigh waves were not observed from events m_b4·3 and m_b4·7 detected at the eastern Kazakh site and one event there of m_b5·0 was totally obscured by interfering Rayleigh waves. The explosions and earthquakes in this region are clearly separated over the entire range of available data, that is, for Rayleigh wave magnitudes down to M_s3·0 and explosion and earthquake *P*-wave magnitudes down to about m_b5·0 and m_b4·2, respectively.

Fig. 7(*c*) compares three explosions from three sites near the Caspian Sea and three explosions from two sites west of the Ural Mountains with 21 earthquakes from the general area of Caucasia–Iran–Turkmen. The three larger Caspian explosions are clearly separated from the earthquake population and have $M_s : m_b$ relationships very similar to the large eastern Kazakh and Novaya Zemlya explosions (this is more clearly illustrated in Fig. 8). The three smaller Ural explosions are closer to the earthquake population and have m_b values significantly lower than eastern Kazakh explosions of equivalent M_s. These anomalies will be discussed in more detail in a

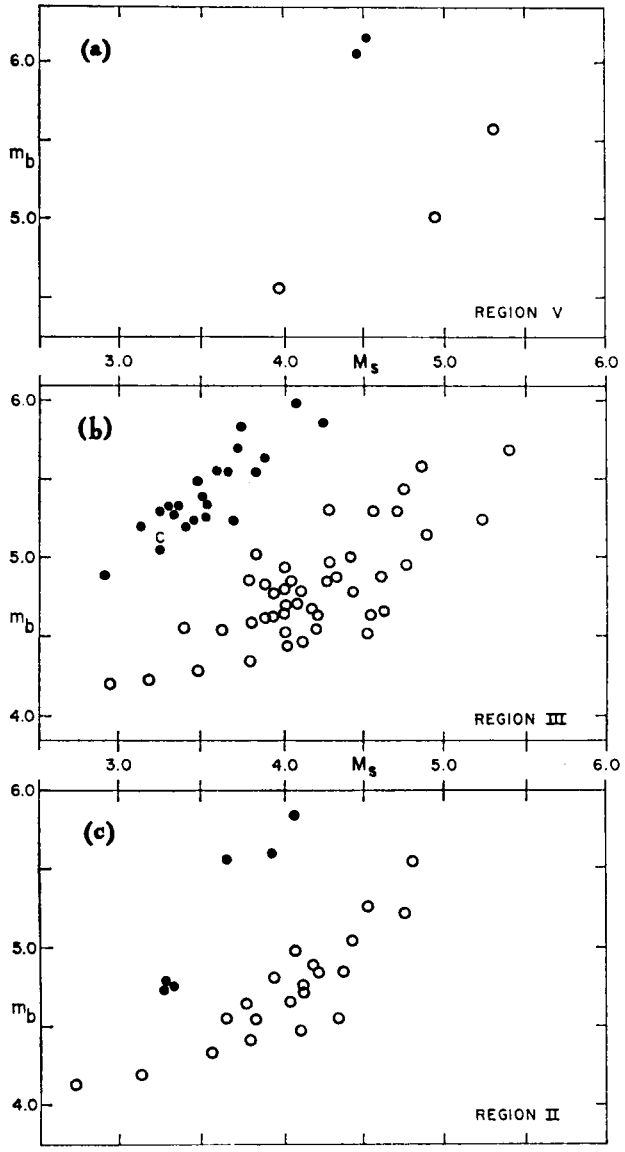

FIG. 7. Regionalized plots of $M_s : m_b$ for Eurasian explosions (solid circles) and earthquakes (open circles). Locations of the events are shown on Fig. 1 and described in the text. The letter, C, denotes the Region III Sinkiang explosion.

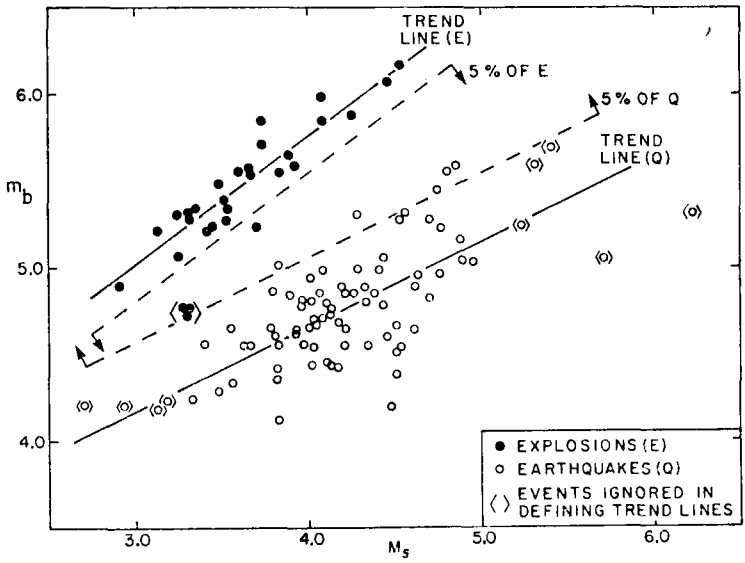

FIG. 8. Combined $M_s : m_b$ plot for all Eurasian events (83 earthquakes and 30 explosions), including the Region I and IV earthquakes. Trend lines are least squares lines defined using all events except those indicated as ignored. Five per cent lines for each population in the direction of the other population are placed at 1·65 standard deviations from the trend line.

later section; here we are illustrating the discrimination capacity of the $M_s : m_b$ criterion for events in the different regions.

To define the discrimination capacity of the $M_s : m_b$ criterion, it is desirable to use data from explosions and earthquakes within similar regions. The data presented here are not ideal in this sense, but it is the best that can be done with the existing geographical distribution of seismic events. In view of the improvements brought about by the new distance and path corrections, however, it is instructive to combine all the Eurasian data.

6.2 *The combined Eurasian data*

All the Eurasian explosions in Fig. 7, with the exception of the Ural events, have a fairly small $M_s : m_b$ scatter with respect to a general trend. Excluding the Ural events, these 27 explosions can be assumed to represent the presently available general explosion trend for Eurasia. The earthquakes, on the other hand, show a significantly greater $M_s : m_b$ scatter than do the explosions. This is because of the variety, orientations and greater complexity of earthquake source mechanisms, the range of source depths and the greater variety of tectonic settings of these earthquakes. But it is worth comparing representative trends of available explosions to conceivable trends and scatter for expected earthquakes. This ignores for the moment the conceivable increased scatter for additional explosions. To illustrate trends and scatter of the two populations, Fig. 8 shows $M_s : m_b$ for all of the Eurasian events (83 earthquakes and 30 explosions). The three Ural explosions are ignored in defining the trend line of the other 'representative' explosions. The four smallest and the five largest M_s earthquakes are ignored in defining the trend line of the earthquakes, the smallest because they may be limited to relatively high m_b earthquakes by the P-wave detection threshold (see Section 7.2), and the largest because they have large scatter and relatively low m_b values, are well separated from the explosions and are in the least difficult magnitude range for discrimination.

The trend line for the explosions is much better defined than for the earthquakes; the average relative $M_s : m_b$ position of the earthquakes appears to be well defined, but a different group of an equivalent number of earthquakes from the same regions could quite likely result in a different slope of the trend line. For reasons given above, these populations do not warrant a detailed statistical study. However, a reasonable probability level for discussion of these events is the 5 per cent level. If the populations are distributed in an approximately normal manner with respect to the trend lines, the two dashed 5 per cent lines in Fig. 8 illustrate the positions of the 5 per cent tails of each population in the direction of the other population. Having excluded the Ural explosions, the remaining 'representative' explosions are clearly separated from the earthquakes at better than the 5 per cent level down to the smallest events plotted; they present no problem in discrimination. A straightforward extrapolation of these trends suggests that a formal overlap at the 5 per cent levels would occur at about $M_s 2{\cdot}1 : m_b 4{\cdot}1$.

An obvious difficulty is encountered with the Ural explosions. They are clearly separated from the small group of regional earthquakes in Fig. 7(*c*), but fall at the 5 per cent level for the perhaps more representative total group of earthquakes in Fig. 8; statistically they are closer to the earthquake than to the remaining explosion population. In terms of discrimination it is worth noting that the separation between the Ural explosions and the Region II earthquakes in Fig. 7(*c*) is very similar to the separation between the USA explosions, Gasbuggy and Rulison, and the south-western North American earthquakes in Fig. 6(*b*). Both can be considered as discrimination in the sense that a decision line can be drawn between the explosion and earthquake populations but they illustrate the difficulty in making a general assertion concerning $M_s : m_b$ discrimination of the Eurasian events. We show later that the different $M_s : m_b$ relationship of the Ural events is more likely due to the source environment rather than the region as a whole. This being the case, it must be assumed that similar effects could result at any of the source regions considered; i.e. a distinction must be made between the clear discrimination achieved for a majority of the available explosions and the conceivable degradation in this discrimination if the source conditions of the Ural events were shown to produce similar results at other sites.

7. Eurasian thresholds

7.1 *Rayleigh wave detection threshold*

In order to discuss the thresholds of discrimination using the $M_s : m_b$ data illustrated in the previous figures, we need to define the detection thresholds of the Rayleigh and *P* waves required and the degree of success of the discriminant (the separation between populations) at these thresholds.

The average Rayleigh wave detection threshold for events in these Eurasian regions is easily defined using the WWSSN stations. Fig. 9 shows a plot of the average number of Rayleigh wave detections per event (for earthquakes and explosions) as a function of M_s, omitting all events with partially and totally obscured Rayleigh waves. The maximum number of detections, near $M_s 5{\cdot}0$, is equivalent to the average number (about 30) of available records per event and is an indication of the operational status of the network. Above $M_s 5{\cdot}0$ the number of detections remains approximately constant but the number of useful measurements drops as the Rayleigh waves become overloaded on the more sensitive stations. Below $M_s 5{\cdot}0$ the number of Rayleigh wave detections per event decreases in a roughly linear manner, approaching zero near $M_s 2{\cdot}7$. This is a gross average representation because it combines both earthquakes and explosions from the different regions, which are located at varying average distances from the groups of central stations (see Fig. 1), but it is a useful illustration of the average capacity of these stations for detecting Rayleigh waves in Eurasia.

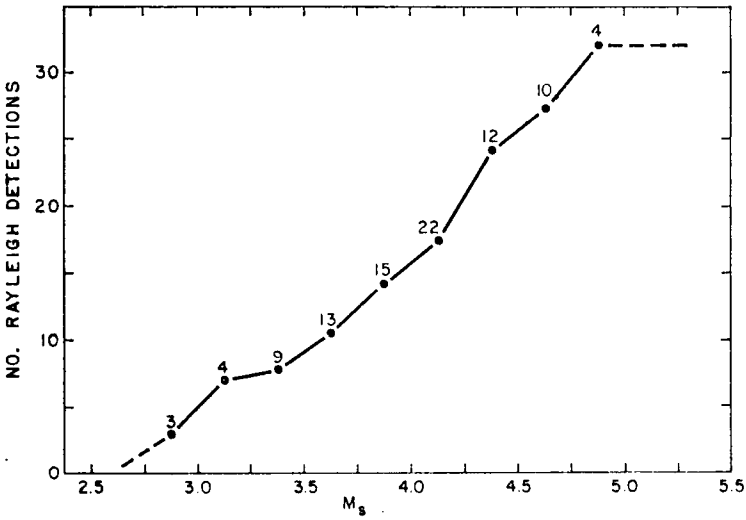

FIG. 9. Average number of WWSSN station Rayleigh wave detections per event (earthquakes and explosions combined) versus M_s. Numbers above points represent the number of events included in each 0·25 M_s interval. Partially obscured events are omitted.

We can apply the interval probability procedures of Basham & Whitham (1971) directly to this curve to define the equivalent Rayleigh wave detection threshold. There will be a 90 per cent probability of detecting the event Rayleigh waves at four or more stations when the mean number of detections is 6·7. As can be seen from Fig. 9, this occurs at about M_s3·2. This is the M_s value we have adopted for the Rayleigh wave detection threshold for Eurasian earthquakes and explosions for the stations employed.

7.2 *P-wave detection (event location) thresholds*

The cumulative number of 1969 earthquakes employed here versus m_b suggests that NOS has a 90 per cent probability of locating an earthquake of about m_b4·7 and greater in these regions of Eurasia. NOS requires at least five *P*-wave detections in order to calculate an epicentre. Below m_b4·7, the percentage of expected earthquakes located decreases very rapidly. The *P*-wave measurements made in this study show that the 42 Eurasian stations would not improve on this, since most of the key stations reporting Eurasian *P* arrivals to NOS are outside of the Eurasian continent. But the m_b4·7 detection and location level does not at present restrict the definition of the explosion $M_s : m_b$ trends in the critical magnitude range, for using the trend lines of Fig. 8, the equivalent m_b value at the M_s3·2 Rayleigh wave detection threshold is about m_b5·2 for the explosions; however, it is about m_b4·3 for the earthquakes.

The most clearly defined earthquake occurrence relationships available for low magnitude earthquakes in these regions of Eurasia are those defined by Anglin (1971) in conjunction with his Yellowknife array (YKA) detection statistics. Using Anglin's occurrence slopes (*b*-values), we estimate that NOS has located approximately 20 per cent of the 1969 earthquakes in these regions in the magnitude range m_b4·2 to m_b4·7. Too much significance cannot be attached to the exact percentage because it depends critically on the m_b range chosen for illustration and on the relative sizes of single array and network m_b values. However, this estimate is sufficiently accurate to show that a significant number of earthquakes in this critical magnitude range are unavailable to a study of this kind, using NOS as a source of events, because of the limitations on the *P*-wave data voluntarily supplied to that agency.

The existing array facilities could assist in the location of more earthquakes in this critical range, not by single- or even multi-array location of events, which are relatively inaccurate (see, for example, Weichert 1969), but by using their signal enhancement capabilities to report arrival times of more small P waves to a central epicentral location agency. Anglin (1971) illustrates for YKA, for example, a 90 per cent cumulative P-wave detection probability at $m_b4{\cdot}0$ for these regions of Eurasia. From information available in various technical reports, some arrays are expected to be more sensitive (e.g. in USA and Norway) and some less sensitive (e.g. in the UK, India, Australia and Sweden) than YKA (see also Basham & Whitham 1971). Therefore, in principle, the capability exists, using the arrays in addition to the more sensitive standard stations, to detect and locate a high percentage of all Eurasian (and world-wide) earthquakes in the $m_b4{\cdot}2$ to $4{\cdot}7$ range. Until this is achieved routinely, or a special study is made of the detection and location of small earthquakes for a period of, say, one year for these regions of Eurasia, we can only assume that the earthquake scatter and trend lines can be extrapolated to the lower levels. The small earthquakes that are in the $M_s2{\cdot}7$–$3{\cdot}5$ range on Fig. 8 are expected, therefore, because of P-wave detection limitations, to be earthquakes with relatively large m_b values for this M_s range; i.e. we would expect few additional earthquakes of, say, $m_b4{\cdot}5$–$4{\cdot}7$ to appear in this low M_s range.

7.3 *Eurasian discrimination threshold*

A suite of earthquakes in this critical magnitude range (55 earthquakes in the ranges $M_s2{\cdot}7$–$3{\cdot}5$, $m_b3{\cdot}6$–$4{\cdot}7$) were studied by Evernden *et al.* (1971) using multi-station teleseismic m_b values and single-station (the high-gain Ogdensburg long period) 20-s M_s values. Their general earthquake $M_s : m_b$ trend agrees well with the trends for North America and Eurasia found here, but the scatter is slightly larger, due probably to the single-station M_s and a lack of path corrections of the type we have employed. The important point is that a great majority of these earthquakes in the $M_s2{\cdot}7$–$3{\cdot}5$ range have m_b values in the range $m_b3{\cdot}8$–$4{\cdot}3$, i.e. fall significantly lower in m_b than the small magnitude Eurasian earthquakes available to this study. Thus, the extrapolation of the earthquake trend in Fig. 8 is probably a conservative, pessimistic one, with the small Eurasian earthquake trend more likely to retain the clear separation from explosions found for the larger magnitudes.

These two considerations, the relatively large m_b values of available small earthquakes due to P-wave detection (event location) limitations, and low m_b values of the Evernden *et al.* earthquakes in the low M_s range, allow us to predict with some confidence that the low magnitude earthquake trend in Fig. 8 is a pessimistic one and that when more earthquake data are available a clear separation between populations will remain at least down to the $M_s3{\cdot}2$ Rayleigh wave detection threshold, and probably much lower. Thus, we accept $M_s3{\cdot}2$ as the discrimination threshold of these Eurasian WWSSN stations for events in the regions defined. It will, however, be important to confirm that the trend for the explosions shown in Fig. 8 continues to lower magnitudes. A definitive study of more Eurasian explosions below $m_b5{\cdot}0$ (additional smaller explosions are available for the years prior to 1968) will require a Rayleigh wave detection capability at a lower threshold than that of the stations employed here.

8. Comparison of North American and Eurasian events

8.1 *Explosion comparisons*

The improvements described in Section 4 were designed so that maximum amplitude Rayleigh waves at any period within the standard long period seismograph pass band will yield magnitudes (M_s) that are independent of the large first order effects of

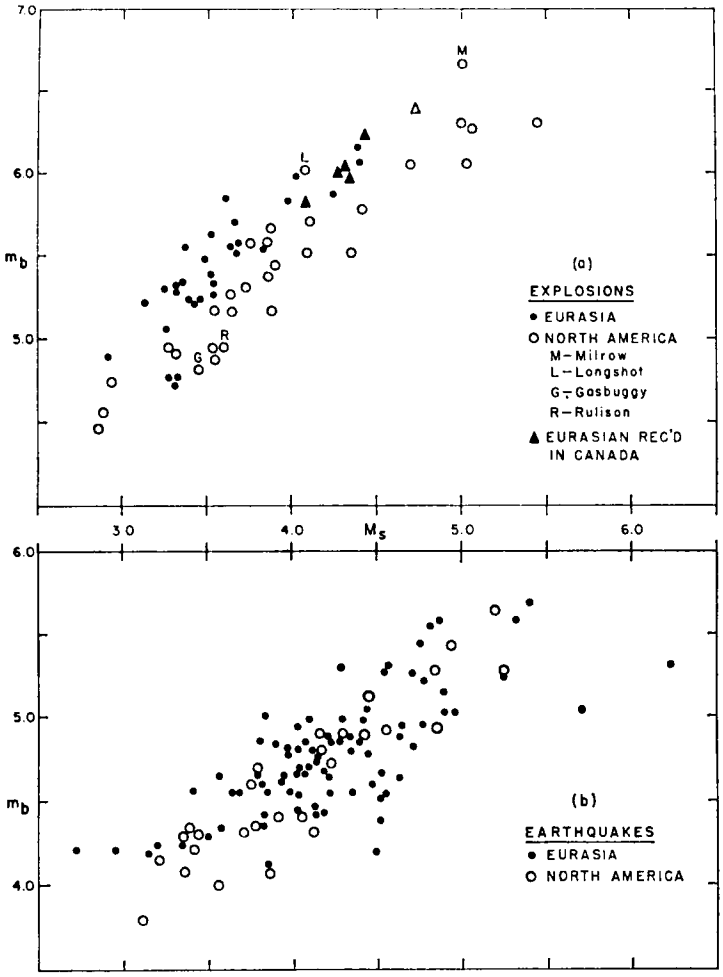

FIG. 10. Combined $M_s : m_b$ plot of (a) all previously discussed explosions and (b) all previously discussed earthquakes. Eurasian explosions from Fig. 7 have M_s depth corrections (if any) removed when plotted here. Six Eurasian explosions defined using data recorded only in Canada are added to the explosion plot for purposes described in the text.

the propagation path. M_s has been shown to reduce $M_s : m_b$ scatter and improve discrimination for North American events, and to reliably discriminate Eurasian events. Now we combine the data from both continents and examine residual differences in $M_s : m_b$ relationships within the general earthquake and explosion populations.

All earthquake and explosion data that have been described previously are plotted as two separate populations in Fig. 10. The Eurasian explosions from Fig. 8, when replotted in Fig. 10(*a*), have depth corrections removed; these were retained in Fig. 8 only to maintain a uniform M_s computational procedure for all events when considering discrimination. The depth corrections are not available for any of the explosion data obtained in previous studies, and in any case, any explosions identified as such by the methods described should subsequently have their M_s values reduced to the shallow focus (h less than about 5 km) equivalent. Fig. 10(*a*) also includes six Eurasian explosions (three at Novaya Zemlaya and three at eastern Kazakh) recorded in

Canada (Basham 1969b) with M_s values recomputed using the refined M_s formula and applying the 'mixed path' corrections from Table 2. The validity of the path corrections is confirmed by these six explosions; they conform in $M_s : m_b$ relationship to explosions of similar magnitudes recorded in Eurasia and suggest a linear continuance of the trend of the smaller explosions. The value of using Rayleigh wave records from the nearest possible stations is also clear from these data; the Rayleigh wave detection threshold for Eurasian earthquakes and explosions using Canadian standard stations is about $M_s 4{\cdot}3$, or about one magnitude unit larger than the equivalent threshold using the Eurasian stations.

The Aleutian explosions, Long Shot and Milrow, which are on the edge of the population of other USA explosions in Fig. 6(*b*), agree very well with the trend of the large Eurasian explosions in Fig. 10(*a*), but, with the exception of the three Ural explosions, Eurasian explosions over the entire range tend to plot significantly above the continental USA explosions.

Explosion m_b values have been shown to depend critically on the detonation rock type and on the degree of water saturation at the detonation point (see, for example, the m_b : yield summary curves presented by Evernden & Filson (1971), but numerous additional and perhaps equally important effects remain to be clearly evaluated. A general phenomenon, which can equally affect earthquake m_b values, is the apparent dissipation of P energy in the upper mantle for some source regions described by Evernden & Clark (1970). Another is unknown network bias, for example, a possible few tenths difference in the m_b base between Canadian values for NTS explosions and NOS values for Eurasian explosions. How much these effects are contributing to the different $M_s : m_b$ positions of NTS and general Eurasian explosions in Fig. 10(*a*) is unknown.

For explosions at a particular site or in a particular medium, the validity of the generally assumed scaling laws, linear scaling of amplitude and cubed-root scaling of dominant frequency with yield, and the proper means of accounting for the scaling in defining accurate relative m_b values is not well understood. In addition, the effects of the explosion depths and, in particular, the effect on m_b of destructive or constructive interference of the free surface reflection, are difficult to account for in general studies. All of these phenomena are important to explosion discrimination on the basis of magnitudes and require extensive research effort.

Recent studies related in the main to single test sites (Ericsson (1971) and Evernden & Filson (1971)) have demonstrated that M_s is a more stable indicator of explosion yield than is the previously employed m_b. This is because M_s is shown to be less sensitive than m_b to the properties of the explosion environment and shows smaller variance when averaged over a number of stations. We can add, as discussed in Section 3.5, that M_s will also be less sensitive to the explosion depth effects described above. With the M_s improvements derived here, and particularly with the path corrections, the M_s scale should now also be a more accurate comparitor of explosions at different test sites. However, we make no claim of the complete absence of source, region and network biases in M_s, only that they are now less important than in m_b.

Thus, explosion differences in Fig. 10(*a*) are more likely to be due to variations in m_b for the different environments and regions. For the USA explosions in Fig. 10(*a*), a majority of the NTS explosions were detonated in tuff, the Aleutian explosions in andesite, and Gasbuggy and Rulison in shale. The large m_b values of the eastern Kazakh, Novaya Zemlya and Caspian explosions indicate a very competent detonation medium and probably a high Q upper mantle structure; the Novaya Zemlya medium is probably a competent limestone and Kazakh and Caspian media probably a competent crystalline basement rock or salt. The $M_s : m_b$ relationship for the three Ural explosions is very similar to that of Gasbuggy and Rulison. They are located in the sedimentary sequences near the Ural Mountains and, like the USA tests, they may have been detonated for natural gas extraction by fracturing of the shale reservoir

medium. The low m_b values of these five sedimentary medium explosions could be partly due to the effect of the separation of the free surface reflection from the primary P wave when containment is unusually deep.

An empirical fit of the M_s values of 16 of the USA explosions in Fig. 10(*a*) with yields for these explosions reported by Springer & Kinnaman (1971) results in the relationship $M_s = 1{\cdot}2 \log Y + 1{\cdot}6$. The mean error in yield that would result from the application of this equation to these 16 explosions is 33 per cent. Assuming a general validity to the arguments above of the stability of M_s with respect to detonation environment, the application of this equation to the Eurasian explosions would result in yields of similar accuracy. For example, the yields of the three Ural explosions would be 279± kt; Gasbuggy & Rulison are reported by Springer & Kinnaman (1971) as having yields of 29 and 40 kt respectively. Applying this formula directly, the $M_s 3{\cdot}2$ discrimination threshold (see Section 7.3) is equivalent to about 20 kt (22±7 kt).

8.2 *Earthquake comparisons*

In contrast to the observed differences between Eurasian and North American explosion data, the Eurasian and south-western North American earthquake populations shown in Fig. 10(*b*) have no large differences in $M_s : m_b$ trends. The source depth corrections applied to the Eurasian earthquakes are not available for the North American earthquakes, but earthquakes in these regions of the south-western United States and north-western Mexico are usually shallow (h less than about 20 km) and any depth corrections would be small (averaging about $M_s 0{\cdot}1$). Thus, the similarities in the average $M_s : m_b$ trends for the two earthquake populations suggests similarities in the average temporal and spatial source conditions in the two regions, and the similarities in degree of scatter in the two populations suggests similar perturbations from average conditions.

We will not review the voluminous literature on conditions at the earthquake source, but it is worthwhile to consider briefly the earthquakes with relatively large m_b that present the greatest problems to discrimination. Wyss & Brune (1968) studied various properties of numerous earthquakes in the same regions of south-western North America and attributed differences in surface wave excitation to regional differences in tectonic stress. In considering this phenomena in terms of apparent source dimensions, they found that the earthquakes in the northern Baja California and Nevada–Arizona regions would have properties most nearly approaching those of explosions. Two earthquakes from northern Baja California are included in the North American earthquakes in Fig. 10(*b*); they have among the largest m_b values relative to M_s. Six earthquakes from the Nevada–Arizona region are also included, but these have $M_s : m_b$ relationships that scatter among the other earthquakes. A range of properties similar to those described by Wyss and Brune can probably be attributed to the Eurasian earthquakes, although near-field observations similar to those available in south-western North America would be required to define them in the same detail. A region with relatively large m_b earthquakes, which includes the earthquakes $M_s 3{\cdot}8 : m_b 5{\cdot}0$ and $M_s 4{\cdot}3 : m_b 5{\cdot}3$ slightly separated from the remaining population in Fig. 10(*b*), appears to be the region along the Tibet–India border along the southern edge of the Himalaya Mountains.

The confidence that can be placed in the $M_s : m_b$ discriminant described for these regions in previous sections is wholly dependent on the assumption that the populations of earthquakes are fully representative of the possible range of $M_s : m_b$ conditions. Although we believe this assumption to be valid, we cannot explicitly define the probability that the discriminant will be successful near the $M_s 3{\cdot}2$ threshold because of the lack of knowledge of the $M_s : m_b$ distribution of the large numbers of earthquakes not reported at the lower magnitudes. It again can be emphasized that the population

of explosions did not include sufficient events near the M_s3·2 threshold to define the explosion trend clearly at and below this magnitude.

9. Conclusions

The purpose of this study has been two-fold: to improve on previously employed M_s computational methods, for both general studies and specific application to earthquake–explosion discrimination, and to define the discrimination capacity of the Eurasian WWSSN stations for seismic events in Eurasia.

The derivation of the Rayleigh wave amplitude envelopes for the four general propagation paths has shown that if Rayleigh wave measurements are restricted to 20-s waves, for any general path whose length is greater than about 25°, the previously employed M_s computational procedures such as Gutenberg's M_s^G or the Prague M_s^P will yield M_s values for earthquakes or underground explosions of sufficient accuracy for intercomparison of events in different regions. The largest relative difference at 20 s due to path alone will be about 0·2 in M_s. The situations at which much larger differences can arise, and for which we found it necessary to devise the described improvements, are those of regional epicentral distances ($\Delta < 25°$), particularly for continental path propagation, and the related phenomenon of having maximum seismogram amplitudes at periods significantly different (usually shorter) than 20 s. The path corrections derived for the four different general paths are gross averages and we prefer to describe them as ' first-order ' corrections; the possibilities of making further refinements of these corrections are numerous: for specific path segments in Eurasia and North America and for different mixed continental-oceanic and purely oceanic situations. What other workers may wish to do in this respect will depend on the requirements of their research.

We do not advocate that agencies which routinely compute magnitudes necessarily adopt the computational procedures described here; they are unnecessary for computations of 20-s magnitudes and for other periods the appropriate path corrections are not available for any specific global path. However, we make a strong appeal to those agencies that publish raw Rayleigh wave measurements to do so in sufficient detail to allow workers to compute M_s using this or any other computational procedure; i.e. in the form of ground amplitude and period of the maximum observed motion, amplitudes at periods near 20 s and, where possible, for periods of other dominant energy in the seismogram.

It is concluded from the analysis of the Eurasian earthquakes and underground explosions that discrimination can be achieved down to a threshold of M_s3·2 using visual measurements from the WWSSN seismograms. This threshold is defined at a level for which there is a 90 per cent probability of observing the required Rayleigh waves on the records of four or more stations, but ignores the ever-present possibility of having the Rayleigh waves partially or totally obscured by an interfering event. (Seventeen per cent of the events selected for analysis were partially or totally obscured by an interfering large earthquake.) The reduction of the North American and Eurasian M_s values to the same absolute base permits an extrapolation to the Eurasian explosions of the M_s versus yield relationship defined on the basis of announced NTS yields. The result of this is an estimate that the M_s3·2 discrimination threshold is equivalent to an Eurasian nuclear explosion of about 20 kt fully contained in hard rock. This fixed M_s absolute base has also isolated residual differences between groups of events on the $M_s : m_b$ plots, differences that are now attributed mainly to m_b, although no detailed attempt has been made here to interpret the specific causes of the m_b differences among events of the same M_s.

A clear distinction should be made between this evaluation of $M_s : m_b$ discrimination of available Eurasian events and the application of the method to discrimination in a Test Ban situation. The majority of explosions employed here show a clearly

defined trend well separated from the earthquake population. The three Ural explosion exceptions must, however, be assumed to represent conceivable $M_s : m_b$ trends for any future test site.

A serious restriction on further studies of discrimination of Eurasian events to lower thresholds will be the general availability of earthquake occurrence information. It is readily apparent from earthquake occurrence curves available in the literature that numerous earthquakes larger than the M_s3·2 discrimination threshold occurred within the regions and time period covered, but were not available from the earthquake information source employed, the NOS lists; only a very small percentage of earthquakes below the discrimination threshold were available. Thus, in general, the discrimination threshold is lower than the only routinely achieved (within periods of a month or so of the events) earthquake location threshold. This, of course, has broad implications with respect to underground test ban control that are outside the scope of this paper. It can be simply stated, however, that any more detailed study of $M_s : m_b$ discrimination at and below the M_s3·2 threshold will require an independent capability for detecting and locating the events of interest.

Acknowledgments

This research was carried out at the Earth Physics Branch, Department of Energy, Mines and Resources, Ottawa, Canada. P. D. Marshall would like to acknowledge the financial support provided by the Canadian Department of External Affairs and the material support of the Department of Energy, Mines and Resources.

We would like to thank Dr K. Whitham and Dr H. I. S. Thirlaway for their useful discussions with us and for the helpful suggestions and criticism during preparation of this paper, and Dr H. S. Hasegawa, Mr F. M. Anglin and Dr G. G. R. Buchbinder for critical comments on the draft manuscript.

P. D. Marshall:
U.K.A.E.A., Blacknest
Brimpton
Reading, RG7 4 RS
Berkshire

P. W. Basham:
Seismology Division
Earth Physics Branch
Department Energy, Mines and Resources
Ottawa, Canada, K1A 0E4

References

Anglin, F. M., 1971. Detection capabilities of the Yellowknife seismic array and regional seismicity, *Bull. seism. Soc. Am.*, **61**, 993.

Basham, P. W., 1969a. Canadian magnitudes of earthquakes and nuclear explosions in southwestern North America, *Geophys. J. R. astr. Soc.*, **17**, 1.

Basham, P. W., 1969b. Canadian detection and discrimination thresholds for earthquakes and underground explosions in Asia, *Can. J. earth Sci.*, **6**, 1455.

Basham, P. W., 1971. A new magnitude formula for short period continental Rayleigh waves, *Geophys. J. R. astr. Soc.*, **23**, 255.

Basham, P. W. & Halliday, R. J., 1970. Canadian seismic data for project Rulison. *Seis. Series Dom. Obs.*, 1969–4, Dept. of Energy, Mines & Resources, Ottawa.

Basham, P. W., Weichert, D. H. & Anglin, F. M., 1970. An analysis of the Benham aftershock sequence using Canadian recordings, *J. geophys. Res.*, **75**, 1545.

Basham, P. W. & Whitham, K., 1971. Seismological detection and identification of underground nuclear explosions, *Publ. Earth Phys. Br.*, **41**, 145.

Båth, M., 1952. Earthquake magnitude determination from the vertical component of surface waves, *Trans. Am. geophys. Un.*, **33**, 81.

Brune, J. N., 1962. Attenuation of dispersed wave trains, *Bull. seism. Soc. Am.*, **52**, 109–112.

Carpenter, E. W. & Marshall, P. D., 1970. Surface waves generated by atmospheric nuclear explosions, United Kingdom Atomic Energy Authority, *AWRE Rept. No.* 088/70. H.M.S.O. London.

Ericsson, U., 1971. A linear model for the yield dependence of magnitudes measured by a seismograph network, *Geophys. J. R. astr. Soc.*, **25**, 49–69.

Evernden, J. F., 1971. Variation of Rayleigh-wave amplitude with distance, *Bull. seism. Soc. Am.*, **61**, 231.

Evernden, J. F. & Clark, D. M., 1970. Study of teleseismic P, II-amplitude data, *Phys. Earth Planet. Int.*, **4**, 24.

Evernden, J. F. & Filson, J., 1971. Regional dependence of surface-wave versus body-wave magnitudes, *J. geophys. Res.*, **76**, 3303.

Evernden, J. F., Best. W. J., Pomeroy, P. W., McEvilly, T. V., Savino, J. M. & Sykes, L. R., 1971. Discrimination between small-magnitude earthquakes and explosions, *J. geophys. Res.*, **76**, 8042.

Ewing, W. M., Press, F. & Jardetzky, W. S., 1957. *Elastic waves in layered media*, McGraw–Hill, New York.

Gutenberg, B., 1945. Amplitudes of surface waves and the magnitudes of shallow earthquakes, *Bull. seism. Soc. Am.*, **35**, 3.

Lambert, D. G., Von Seggern, D. H., Alexander, S. S. & Galat, G. A., 1969. The Long Shot experiment, *Air Force Technical Applications Center*, Washington, D.C.

Liebermann, R. C. & Pomeroy, P. W., 1969. Relative excitation of surface waves by earthquakes and underground explosions, *J. geophys. Res.*, **74**, 1575.

Liebermann, R. C. & Basham, P. W., 1971. Excitation of surface waves by the Aleutian underground explosion MILROW (2 October 1969), *J. geophys. Res.*, **76**, 4030.

SIPRI, Stockholm International Peace Research Institute, 1968. Seismic methods for monitoring underground explosions, rapporteur D. Davies, Almqvist and Wiksell, Stockholm.

Springer, D. L. & Kinnaman, R. L., 1971. Seismic source summary for U.S. underground nuclear explosions, 1961–1970, *Bull. seism. Soc. Am.*, **61**, 1073.

Tsai, Y. & Aki, K., 1970. Precise focal depth determination from amplitude spectra of surface waves, *J. geophys. Res.*, **75**, 5729.

Vanek, J., Zatopek, A., Karnik, V., Kondorskaya, N. V., Riznichenko, Y. V., Savarensky, E. F., Solov'ev, S. L. & Shebalin, N. V,. 1962. Standardization of magnitude scales, *Bull. (Izvest.) Acad. Sci. U.S.S.R., Geophys. Ser.*, **2**, 108.

Weichert, D. H., 1969. Epicenter determination by seismic arrays, *Nature*, **222**, 155.

Wyss, M. & Brune, J. N., 1968. Seismic moment, stress, and source dimensions for earthquakes in the California–Nevada region, *J. geophys. Res.*, **75**, 4681.